


RESEARCH

Open Access



# The ankyrin repeat-containing protein PIANK1 mediates mycelial growth, oospore development, and virulence in *Peronophythora litchii*

Junjian Situ<sup>1\*†</sup>, Xinning Zhang<sup>1†</sup>, Xiaofan Zhou<sup>1</sup>, Zijing Zhang<sup>1</sup>, Pinggen Xi<sup>1</sup>, Guanghui Kong<sup>1</sup> and Zide Jiang<sup>1\*</sup> 

## Abstract

Litchi downy blight, caused by *Peronophythora litchii*, is one of the most serious diseases in major litchi-producing regions worldwide. The ankyrin (ANK) repeat is one of the most common protein-protein interaction motifs found in all kingdoms of life proteins. ANK-containing proteins have been demonstrated to regulate various biological processes in animals, plants, and fungi. However, their functions in phytopathogenic oomycetes remain unknown. Here, we identified 284 non-redundant genes that encode ANK-containing proteins in *P. litchii* and classified them into 11 subfamilies. Among them, *PIANK1* was found to be highly up-regulated in oospores and from zoospores to the infection process. Loss of *PIANK1* in *P. litchii* resulted in impaired mycelial growth and cyst germination, accelerated zoospore encystment, and increased sensitivity to hyperosmotic stresses and Congo red. Furthermore, *PIANK1* deletion mutants were defective in oospore formation and development. Inoculation assays showed that the absence of *PIANK1* severely diminished the pathogen's virulence on litchi leaf and fruit. Through transcriptome analysis and nitrogen source utilization assays, we demonstrated that *PIANK1* modulates the pathogen's nitrogen metabolism. Altogether, our findings indicate that *PIANK1* is a key regulator of sexual and asexual development, and virulence in *P. litchii*.

**Keywords** Litchi downy blight, Oomycete, ANK proteins, Oospore, Virulence

## Background

With the rapid accumulation of genomic information, proteins containing repetitive amino acids have drawn significant attention in the last decade. Among these, ankyrin (ANK) repeat is a commonly occurring protein repeat in prokaryotes, eukaryotes, and some viruses (Li et al. 2006). This ANK repeat motif consists of 33 amino acid residues repeated in tandem arrays. These arrays fold cooperatively to create specific secondary and tertiary structures, which are crucial for mediating molecular recognition through protein-protein interactions (Sedgwick et al. 1999; Kumar et al. 2021). The ANK-containing protein was first characterized in yeast and *Drosophila*

<sup>†</sup>Junjian Situ and Xinning Zhang have contributed equally to this work.

\*Correspondence:

Junjian Situ  
Junjian.st@hotmail.com  
Zide Jiang  
zdjiang@scau.edu.cn

<sup>1</sup> Guangdong Province Key Laboratory of Microbial Signals and Disease Control, Department of Plant Pathology, South China Agricultural University, Guangzhou 510642, China



(Breedon et al. 1987) and named after the discovery of this sequence in the cytoskeletal protein ankyrin (Lux et al. 1990). Subsequently, they have been found to be involved in a wide range of functions, including cell cycle regulation, cytoskeleton interactions, signal transduction, and transcriptional control (Al-Khodor et al. 2010; Odon et al. 2018; Sharma et al. 2020; Kolodziej et al. 2021).

In plants, ANK-containing proteins play a vital role in multiple processes, such as growth and development, hormone synthesis, signal transduction, and response to abiotic and biotic stresses. For instance, overexpression of *MdANK2B* increased resistance to salt stress and reduced sensitivity to ABA in both transgenic apple calli and seedlings (Zhang et al. 2021). Besides, it also led to a decrease in the accumulation of reactive oxygen species (ROS) by enhancing the activity of antioxidant enzymes in response to salt stress (Zhang et al. 2021). *GmANK114*, which encodes a protein belonging to the ANK-RF subfamily containing a RING finger (RF) domain in addition to the ankyrin repeats, confers drought and salt tolerance in *Arabidopsis* and soybean (Zhao et al. 2020). Recently, two ankyrin repeat proteins, YrU1 and Lr14a, were found to confer stripe rust and leaf rust resistance in wheat, respectively (Wang et al. 2020; Kolodziej et al. 2021). ANK-containing proteins have also been identified in plant-pathogenic fungi, a few of which are involved in virulence. For instance, TOXE, a transcription factor consisting of four ankyrin repeats from the maize pathogen *Cochliobolus carbonum*, plays a specific regulatory role in cyclic peptide production and the virulence of *C. carbonum* (Pedley et al. 2001). *Fusarium graminearum* FgANK1 is required for host-mediated nitric oxide (NO) production and virulence via interacting with a zinc finger transcription factor FgZC1 (Ding et al. 2020). However, the function of ANK-containing proteins in oomycetes has not been investigated.

Oomycetes are a diverse group of eukaryotic microorganisms with a life cycle and morphologic characteristics similar to filamentous fungi but are evolutionarily related to photosynthetic algae (Beakes et al. 2012; Thines et al. 2014). Phytopathogenic oomycetes, such as downy mildew, *Phytophthora*, *Peronophythora*, and *Pythium*, can cause significant damage to important agricultural crops and natural ecosystems (Kamoun et al. 2015). One of the most serious diseases affecting litchi production and post-harvest is litchi downy blight, which is caused by *Peronophythora litchii* (Zhu et al. 2022). This pathogen attacks fruit, panicles, and leaves. Asexual sporangia and zoospores are the main inoculums of *P. litchii*. In addition, sexual oospores act as resting structures surviving in soil or debris for several years (Situ et al. 2022). While research on gene functions in *P. litchii* has been accelerated with the availability of genome resources and the

development of an efficient CRISPR/Cas9 genome editing system, our understanding of the molecular pathogenesis of this pathogen still lags behind many other phytopathogenic oomycetes (Ye et al. 2016; Situ et al. 2020; Li et al. 2021; Wang et al. 2022).

Here, we have identified 284 non-redundant genes encoding ANK-containing proteins in *P. litchii*, which were classified into 11 subfamilies. Among them, the ANK-PDZ subfamily gene, *PLANK1*, was found to be significantly induced in oospores and from zoospores to infection stages. Subsequent experiments showed that *PLANK1* deletion mutants were defective in vegetative growth, zoospores encystment, cysts germination, stress tolerance, sexual reproduction, and virulence. Through transcriptome analysis and nitrogen source utilization assays, we demonstrated that *PLANK1* mediates the pathogen's nitrogen metabolism. Overall, this study sheds light into the function of ANK-containing proteins in oomycetes development and pathogenesis.

## Results

### Identification of ANK-containing proteins in *P. litchii*

We performed Pfam analysis on all annotated proteins in the *P. litchii* genome and identified a total of 284 genes that encode proteins containing the ANK motif (PF13637) (Table 1 and Additional file 1: Table S1). The number of ANK repeats in a protein ranges from 1 to 31, with an average of 5.6 (Additional file 2: Figure S1). The average size of *PLANK* proteins is 822 amino acids (aa), which is larger than the average size of all predicted proteins (580 aa) in the *P. litchii* genome. The characteristics of *PLANK* proteins are summarized in Additional file 1: Table S1. The 284 *PLANK* proteins were analyzed for additional recognizable protein domains and subsequently classified into 11 clusters of structurally related proteins (Table 1). The subfamily ANK-M contained 144 proteins with ANK domain only, while 4 of the *PLANK* proteins also contained a signal peptide (Additional file 1: Table S1).

To examine the expression pattern of the *PLANK* genes during the infection process, we analyzed the RNA-Seq data of *P. litchii* infection stages. Transcripts of 283 ANK protein-coding genes were detected in at least one infection stage (Fig. 1a). As shown in the heatmap, 13 *PLANK* genes were constantly up-regulated in all the infection stages, while 16 genes were up-regulated at early infection stages (1.5–6 h post-inoculation [hpi]), and 34 genes were up-regulated at late infection stages (12–24 hpi). Meanwhile, 48 genes were constantly down-regulated at all the infection stages, and 72 genes were down-regulated at early or late infection stages. The diverse expression patterns across infection stages might suggest

**Table 1** Number of *P. litchii* ANK-containing proteins in different subfamilies

Subfamily	Description	Number of ANK protein	Average number of ANK repeats
ANK-M	ANK protein with only the ankyrin repeat	144	6.10
ANK-TM	ANK-transmembrane protein	24	5.17
ANK-PK	ANK protein with kinase activity	21	9.14
ANK-ZF	ANK protein with zinc finger domain	13	4.08
ANK-IQ	ANK protein with calmodulin-binding motif	12	2.50
ANK-RF	ANK protein with RING finger domain	7	2.29
ANK-RAS	ANK protein with GTPase of the Ras superfamily	5	4.60
ANK-WW	ANK protein with proline-rich polypeptides binding domain	5	5.40
ANK-PDZ	ANK protein with discs-large homologous regions	4	3.25
ANK-TPR	ANK protein with the TPR	4	3.75
ANK-O	ANK protein with other domains	45	4.73

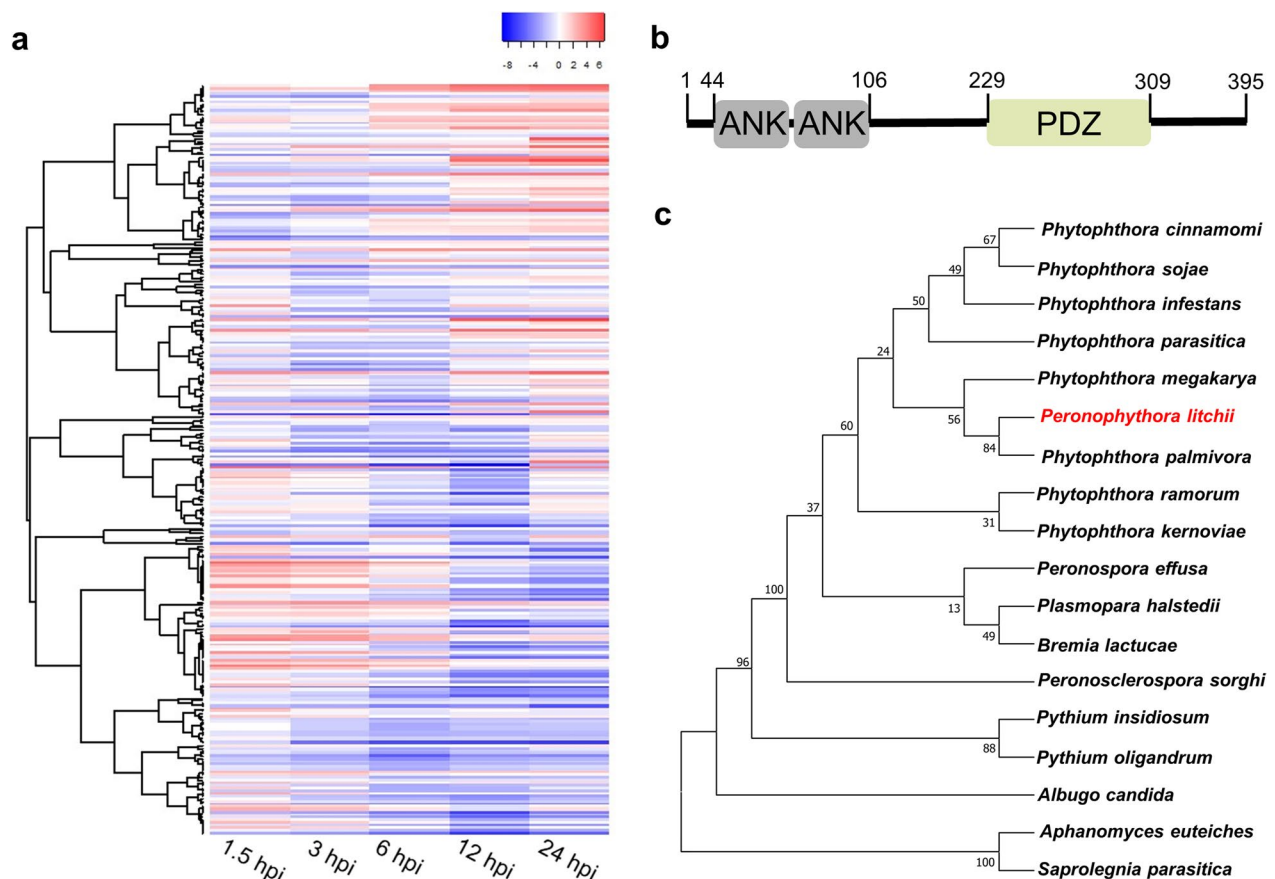


**Fig. 1** Transcriptional analysis of the *PIANK* genes and sequence feature of *PIANK1*. **a** Heatmap of the transcription level of *PIANK* genes in the pathogen infection stages. **b** Sequence characterizations of *PIANK1*. **c** Phylogenetic analysis of *PIANK1* and its homologous proteins in other oomycetes. Phylogenetic dendrograms were constructed by MEGA X with the Neighbor-Joining method using 1000 bootstrap replications

different functional roles of the *PLANK* genes in the infection process.

### Sequence and expression pattern analysis of *PLANK1*

To investigate the function of ANK-containing proteins in *P. litchii*, *PLANK1* was selected for further research because of its higher enrichment in expression during infection stages (Additional file 1: Table S1). The open reading frame of *PLANK1* was 1188 bp in length and contained two introns, resulting in a protein with 395 amino acids. In addition to the two ANK domains, *PLANK1* also possesses a PDZ domain (Fig. 1b). Phylogenetic analysis showed that *PLANK1* is only conserved in oomycetes, suggesting a potentially unique role in these microorganisms (Fig. 1c).

Subsequently, reverse-transcription quantitative PCR (RT-qPCR) was performed to further define the expression pattern of *PLANK1* at different life stages. The results showed that *PLANK1* was highly induced in zoospores, cysts, germinating cysts, and oospores. In addition, the expression of *PLANK1* gradually increased

after inoculation (Additional file 2: Figure S2), which was consistent with the RNA-Seq data. This result suggests that *PLANK1* may play a crucial role during the stage of *P. litchii* development and infection.

### Generation of *PLANK1* knockout and complementation strains in *P. litchii*

To further explore the possible function of *PLANK1*, we generated knockout mutants of the *P. litchii* wildtype (WT) strain SHS3 by the CRISPR/Cas9 genome editing system. A single guide (sgRNA) was designed to disrupt the *PLANK1* gene following the gene replacement strategy schematically displayed in Fig. 2a. Three independent knockout mutants (KO11, KO14, and KO39) were obtained (Fig. 2b–d). We used a transformant as the control (CK) strain in which *PLANK1* had not disrupted. In order to ensure that the observed phenotype of these knockout mutants was caused by the loss of *PLANK1*, the pTOR vector containing HAM34 promoter and *PLANK1* ORF region with a synonymous substitution at the single guide RNA (sgRNA) target site was reintroduced into

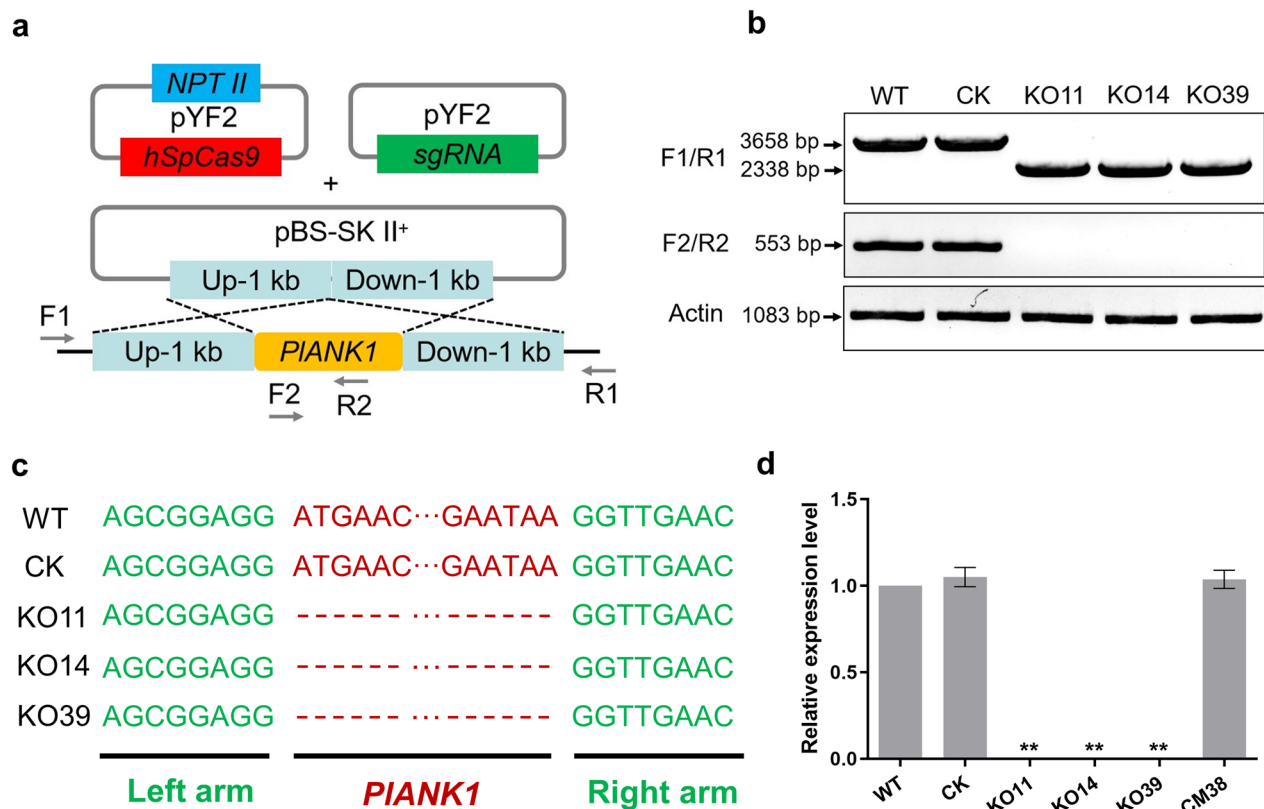


**Fig. 2** CRISPR/Cas9-mediated knockout of *PLANK1*. **a** A single guide RNA targeting the *PLANK1* coding region was designed to disrupt *PLANK1*. **b** and **c** Three independent deletion mutants were identified by genomic PCR and confirmed by sequencing. **d** Relative expression levels of *PLANK1* were determined by RT-qPCR in WT, CK, KO11, KO14, KO39, and CM38. The constitutive expression of *PIActin* was used as a reference gene, and expression levels were normalized using the WT values as 1. Data represent means  $\pm$  SD. The experiment was repeated three times independently. Asterisks denote significant differences between *PLANK1* knockout mutants and the WT (\*\*  $p < 0.01$ )

the mutant strain (KO39) to create a complementation strain. After hygromycin B screening and qPCR verification, the *PLANK1* transcriptional level of the complementation strain CM38 was close to the WT strain SHS3 (Fig. 2d and Additional file 1: Table S2). These results suggested that we had successfully obtained three independent *PLANK1* disruption mutants and a complementation strain for further studies.

#### *PLANK1* contributes to vegetative growth, zoospore encystment, and cyst germination

To investigate the role of *PLANK1* in mycelial growth, the WT, CK, *PLANK1* knockout mutant, and complementation strains were cultured on carrot juice agar (CA) medium. The *PLANK1* knockout mutants showed

a slower growth rate on CA medium compared to the WT, CK, and complementation strains (Fig. 3a, b). To further evaluate whether *PLANK1* contributes to *P. litchii* asexual reproduction and spore development, sporangia yield, zoospore release, encystment, and cyst germination rate of the above strains were examined. The results showed that sporangia yield and zoospore release rate were not significantly different among these strains (Fig. 3c, d). However, compared with the WT and CK strains, zoospores of the *PLANK1* knockout mutants exhibited more rapid encystment at 1 h and 3 h after being released from sporangia, while the complementation strain showed a similar encystment rate to the WT and CK strains (Fig. 3e). Moreover, cyst germination was also impaired by approximately 20%

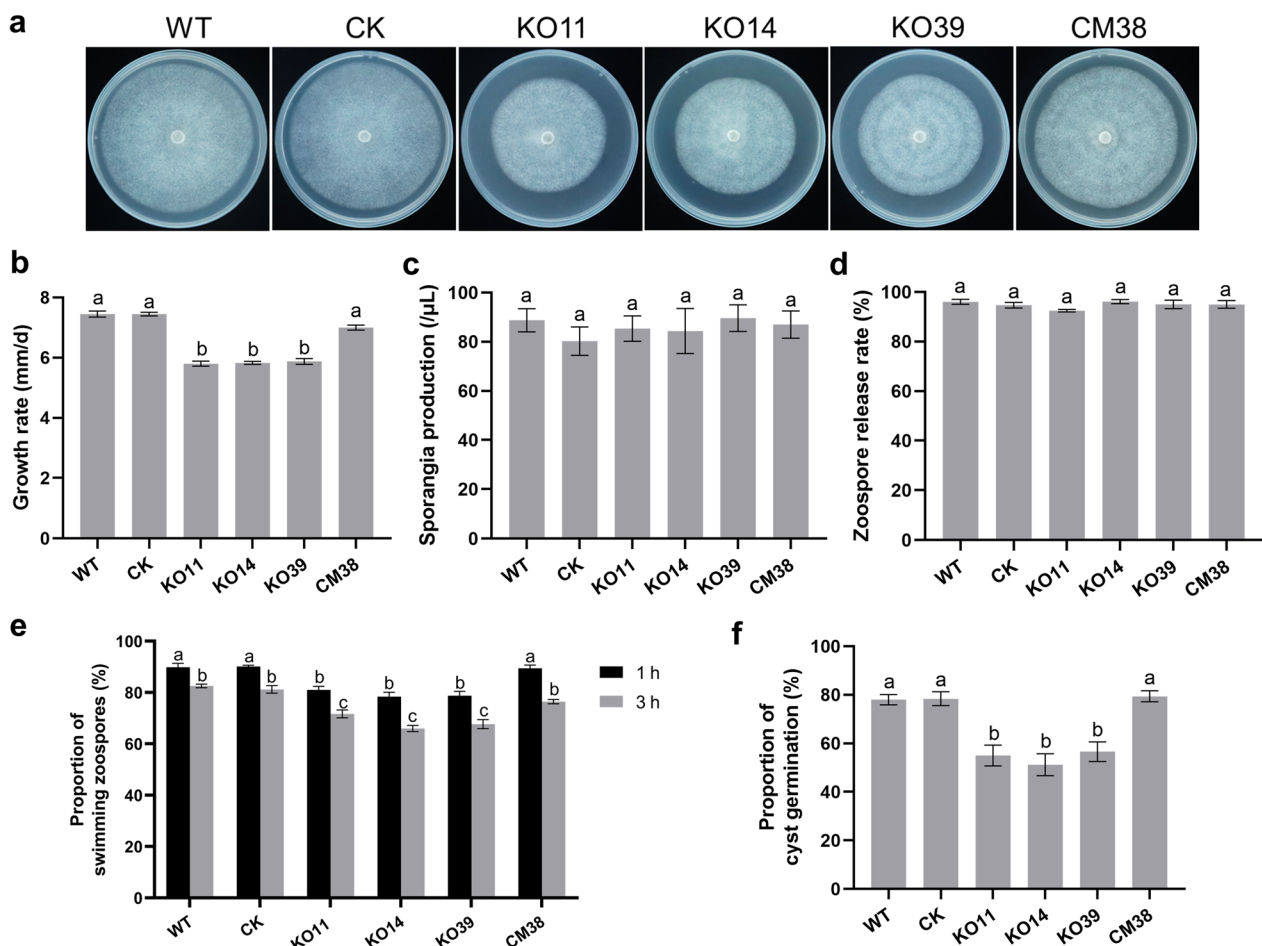


**Fig. 3** Growth rate and asexual reproduction analysis of the *PLANK1* mutants. **a** and **b** The colony growth rate of the WT, CK, *PLANK1* knockout mutant and complementation strains. Photographs were taken at 7 d. The experiment was repeated three times independently, with three technical replications per biological repeat. **c** Mean sporangia number in 1 μL sporangia suspension. **d** Mean zoospore release rate. Sporangia were harvested by flooding the mycelia with the same sterile distilled water. **e** Mean zoospore encyst time. **f** Mean cyst germination rate. For **c** to **f**, the initial concentration of cysts, sporangia, and zoospores was adjusted to be the same for each strain. Data represent means ± SD. All the experiments were repeated three times independently, with three technical replications per biological repeat. Different letters represent significant differences ( $p < 0.01$ ; Duncan's Multiple Range Test)

in the *PLANK1* knockout mutants (Fig. 3f). The above results indicate that *PLANK1* contributes to vegetative growth, zoospore encystment, and cyst germination.

#### ***PLANK1* is involved in the stress responses of *P. litchii***

To explore whether *PLANK1* is involved in stress response, the strains were cultured on Plich media supplemented with different stressors. Compared with the WT, CK, and complementation strains, the *PLANK1* knockout mutants showed a higher growth inhibition rate under hyperosmotic stresses, including NaCl and D-Sorbitol (Fig. 4a, b). In addition, a higher inhibition rate was also observed on plates with Congo red (CR) (Fig. 4a, b). These results showed that *PLANK1* positively regulated the responses to hyperosmotic and CR stresses, suggesting that *PLANK1* is involved in maintaining cell wall integrity and responding to stresses in *P. litchii*.

#### ***PLANK1* knockout disrupts oospore formation in *P. litchii***

To determine the effects of *PLANK1* knockout on oospore development, oospore numbers were calculated in the WT, CK, *PLANK1* knockout mutant, and complementation strains after 7 d and 14 d of growth on CA medium. The *PLANK1* knockout mutants exhibited a significant decline in oospore density after 7 d of growth (Fig. 5a). Although all the strains showed an increase in oospore density after 14 days of growth, the density in the *PLANK1* knockout mutants remained significantly lower than that of other strains (Fig. 5a). Oospore morphology was also observed when mycelia were inoculated in CA medium for 7 d and 14 d. About half of 7-day-old oospores of the *PLANK1* knockout mutants showed decreased amounts of cytoplasm in the oospore compared with the WT, CK, and complementation strains (Fig. 5b, d). The abnormal development of oospores in the *PLANK1* knockout mutants was even more conspicuous after 14 d growth, with the cytoplasm of abnormal oospores appearing fragmented and forming irregularly shaped masses (Fig. 5c, d).

Subsequently, we determined the viability of oospores through methylthiazolyldiphenyl-tetrazolium bromide (MTT) staining. The 7- and 14-day old oospores of the WT, CK, and complementation strains were stained purple (Fig. 5e), indicating that they are viable. However, most of the cytoplasm in the *PLANK1* knockout mutants

were light purple or unstained, suggesting a loss of viability (Fig. 5e). Collectively, these data demonstrated that *PLANK1* is required for the sexual reproduction in *P. litchii*.

#### ***PLANK1* is required for *P. litchii* virulence**

Inoculation assays were performed to determine the role of *PLANK1* in the virulence of *P. litchii*. We inoculated the tender leaves and mature fruit of litchi with 100 zoospores from the WT, CK, knockout mutant, and complementation strains individually. Forty-eight hours post-inoculation, the leaves inoculated with zoospores of the WT, CK, or complementation strains showed typical water-soaked disease symptoms, while the lesions caused by the *PLANK1* knockout mutants were significantly smaller (Fig. 6a, b). The litchi fruit inoculated with the *PLANK1* knockout mutants also exhibited fewer disease symptoms than those inoculated with the WT, CK, and complementation strains (Fig. 6c, d). Similar results were obtained from mycelial mat inoculation assays (Additional file 2: Figure S3). The above results suggest that *PLANK1* plays an important role in the *P. litchii* virulence on litchi.

#### ***PLANK1* is involved in nitrogen assimilation**

To identify the *P. litchii* genes regulated directly or indirectly by *PLANK1*, we performed RNA-Seq to compare the transcriptomes of the WT and two knockout mutants (KO11 and KO39). Our analysis identified a total of 333 differentially expressed genes (DEGs) in the mutants compared to the WT strain, with 75% (250 genes) up-regulated and 25% (83 genes) down-regulated (Additional file 1: Table S3). Gene ontology (GO) analysis showed that the DEGs were mainly associated with the extracellular region, protein serine/threonine kinase activity, signal transduction, cell wall organization, DNA-binding transcription factor activity, and nitrate assimilation (Fig. 7a). KEGG functional enrichment analysis further showed that the DEGs were significantly enriched for several metabolic pathways, including ascorbate and aldarate metabolism, glycerolipid metabolism, nitrogen metabolism, and pentose and glucuronate interconversions (Fig. 7b).

All the DEGs involved in nitrate assimilation showed significant down-regulation in our RNA-Seq data.

(See figure on next page.)

**Fig. 4** *PLANK1* is involved in stress tolerance. **a** Assay of mycelial growth of the WT, CK, and *PLANK1* knockout mutant and complementation strains on Plich media supplemented with 0.05 M NaCl, 0.1 M CaCl<sub>2</sub>, 0.2 M D-sorbitol, 2 mM H<sub>2</sub>O<sub>2</sub>, 100 µg/mL CFW, or 350 µg/mL CR. Images were taken 7 d post-inoculation. **b** Colony diameters were measured 7 d after inoculation. Rates of growth inhibition were calculated for each treatment relative to the growth rate on Plich medium. Data are mean ± SD. The experiment was repeated three times independently, with three technical replications per biological repeat. Asterisks denote significant differences between *PLANK1* knockout mutants and the WT strain (\*\*  $p < 0.01$ )

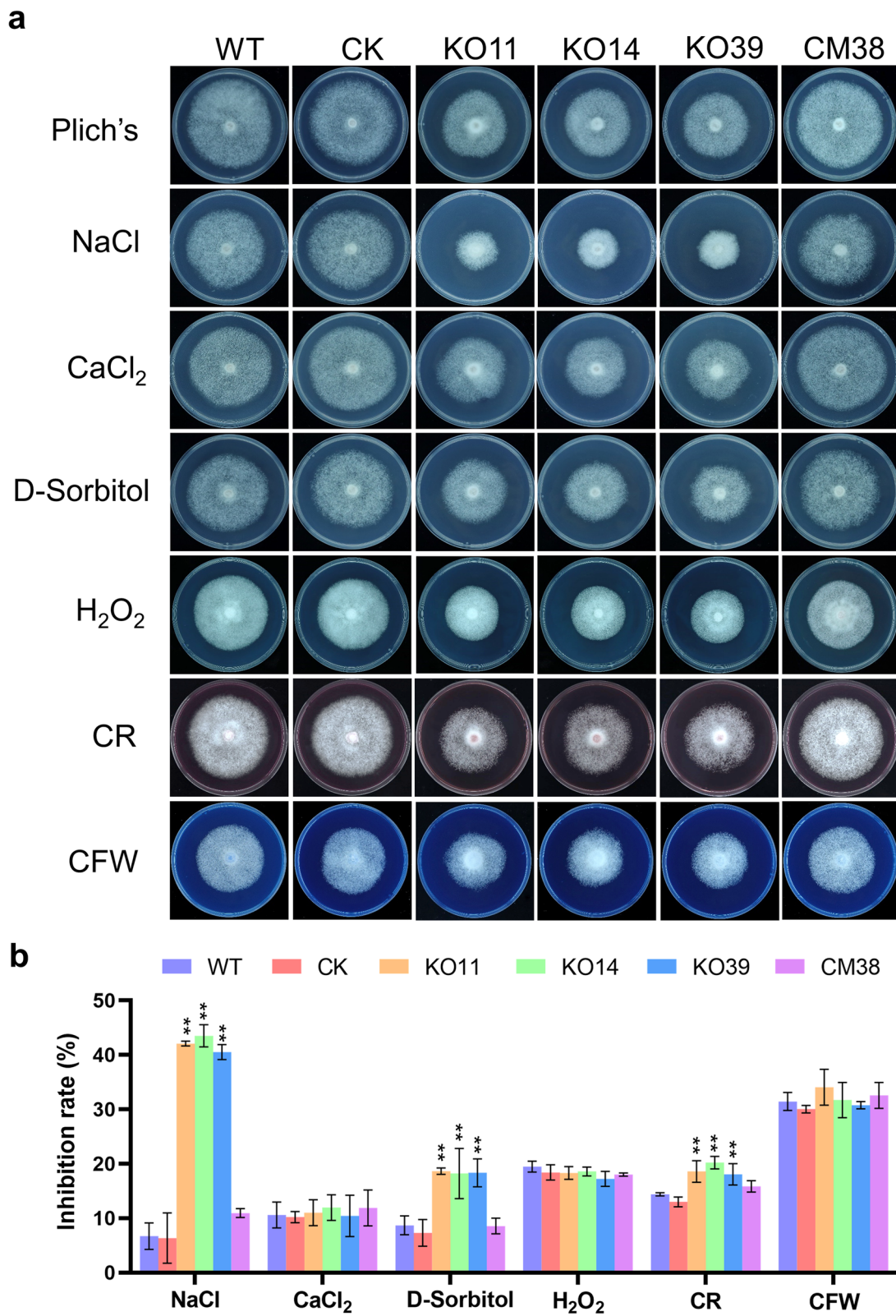


**Fig. 4** (See legend on previous page.)

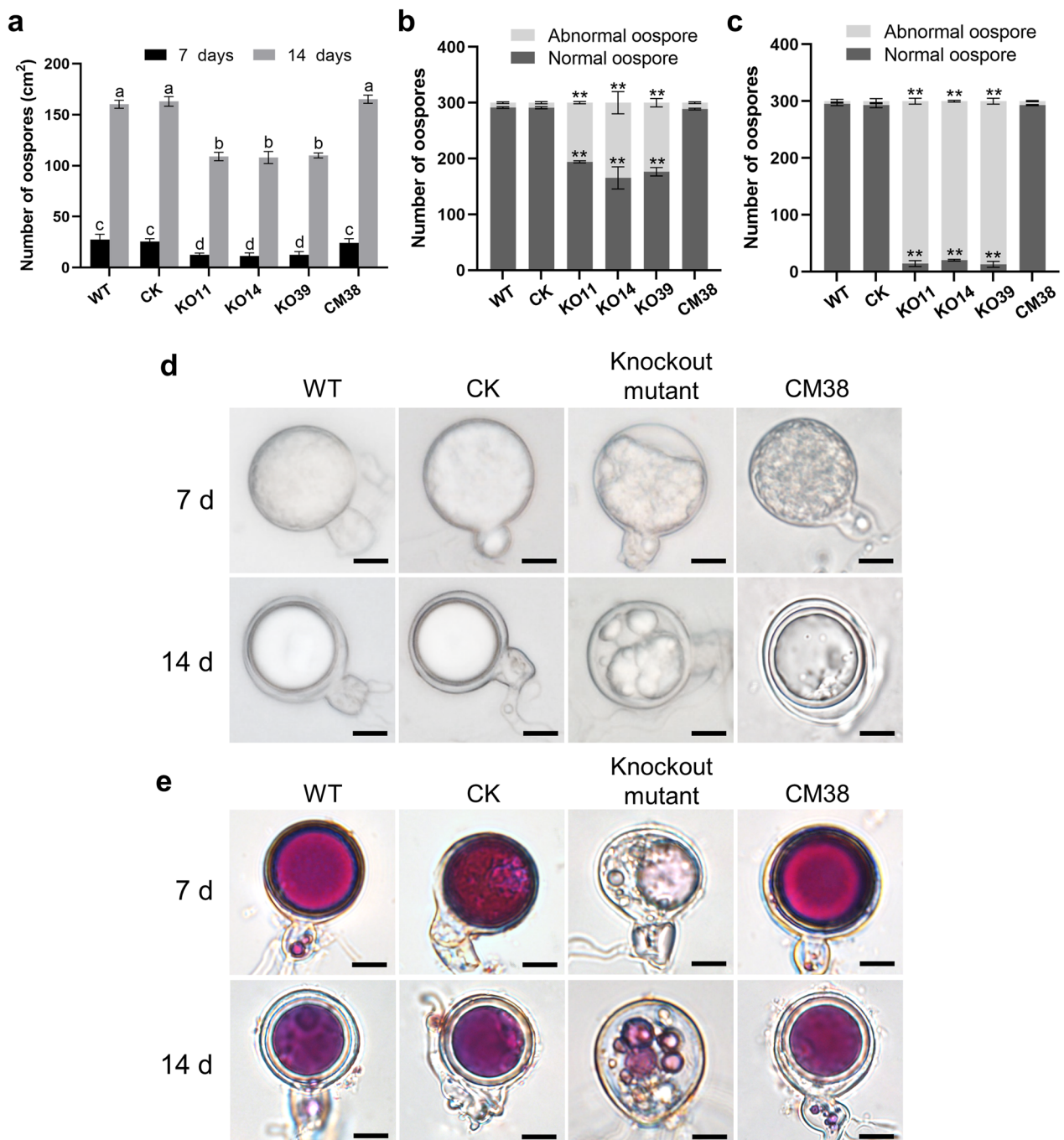


**Fig. 5** Sexual reproduction analysis of the *PIANK1* mutants. **a** Amount of oospores produced by the WT, CK, and *PIANK1* knockout mutant and complementation strains. Different letters represent significant differences ( $p < 0.01$ ; Duncan's Multiple Range Test). **b** Amount of normal and aborted oospores produced by the WT, CK, and *PIANK1* knockout mutant and complementation strains after 7 d cultured in CA. **c** Amount of normal and aborted oospores produced by WT, CK, and *PIANK1* knockout mutants and complemented strain after 14 d cultured in CA. Data represent means  $\pm$  SD. The experiment was repeated three times independently, and asterisks denote significant differences between *PIANK1* knockout mutants and the WT strain (\*\*  $p < 0.01$ ). **d** Morphology of oospores produced in 7- and 14-day-old cultures of the WT, CK, and *PIANK1* knockout mutant and complementation strains. The bars indicate 20  $\mu$ m. **e** Oospores produced in 7- and 14-day-old cultures of the WT, CK, and *PIANK1* knockout mutant and complementation strains treated with tetrazolium bromide (MTT)



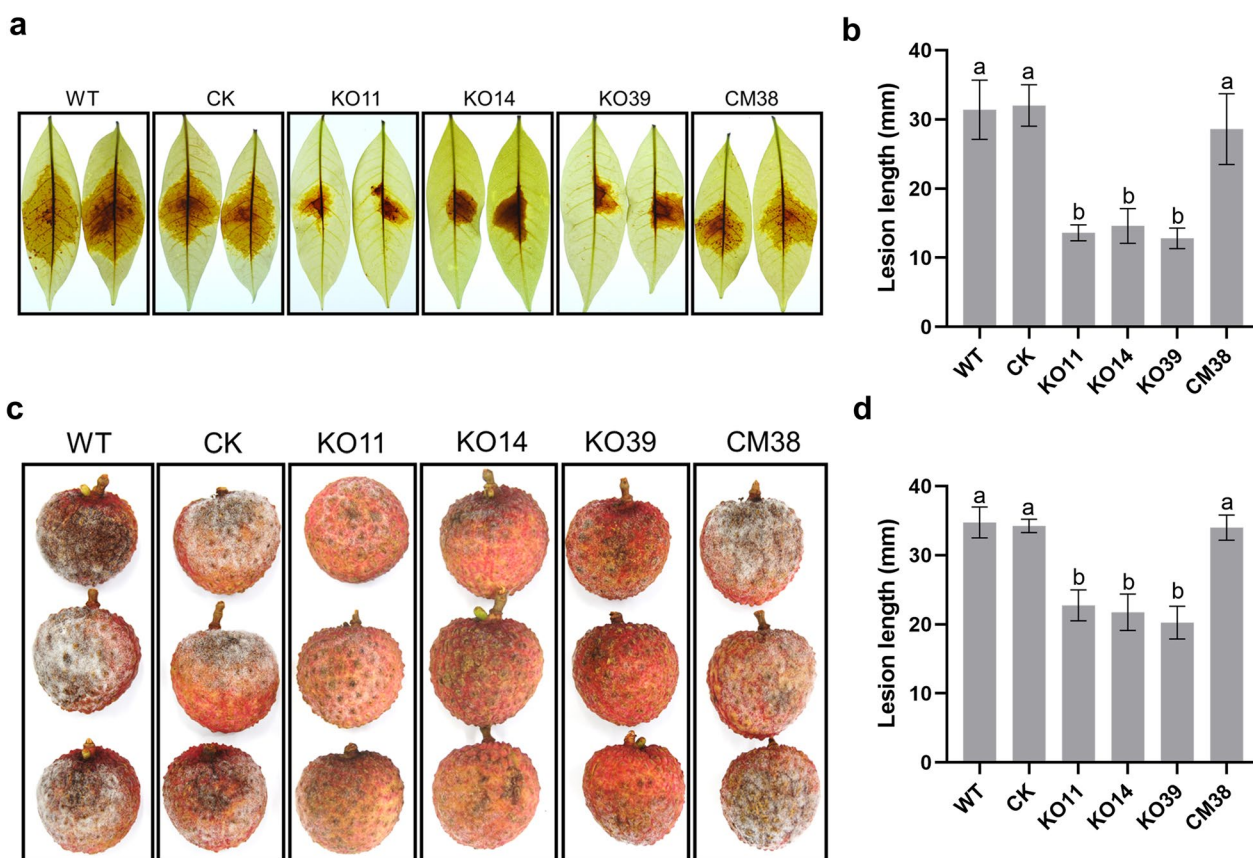


**Fig. 6** Inoculation assay of the *PIANK1* knockout mutants. **a** One hundred zoospores of the WT, CK, and *PIANK1* knockout mutant and complementation strains were inoculated on tender litchi leaves ( $n > 30$  for each strain) for 48 h at 25 °C in the dark. Images are two representatives for each instance. **b** Lesion length measured after 48 hpi. Different letters represent significant differences ( $p < 0.01$ ; Duncan's Multiple Range Test). **c** One hundred zoospores of the WT, CK, and *PIANK1* knockout mutants and complemented strain were inoculated on litchi fruit ( $n > 30$  for each strain) for 72 h at 25 °C in the dark. Images are three representatives for each instance. **d** Lesion length measured after 72 hpi. Different letters represent significant differences ( $p < 0.01$ ; Duncan's Multiple Range Test). Experiments were repeated three times independently

Nitrogen sources are essential for microbes to carry out vital functions, such as energy generation and protein synthesis, which are necessary for rapid growth, niche colonization, and infection (Tang et al. 2020). Therefore, the nitrate/nitrite transporter encoding genes *PINRT1* and *PINRT2* and the nitrite reductase encoding gene *PINiR1* were selected for further analysis. We examined the expression patterns of each down-regulated gene in vegetative mycelia using RT-qPCR, and the results were consistent with the RNA-Seq data (Additional file 2: Figure S4), suggesting the involvement of *PIANK1* in nitrogen metabolism. We also tested the expression patterns of the above genes in the early (6 hpi) and late (12 hpi) infection stages, respectively. The expression levels of *PINiR1* in the infection stages were not significantly different between the *PIANK1* knockout mutants and the WT strain (Additional file 2: Figure S4). The expression of *PINRT1* was down-regulated in the early infection stages in the *PIANK1* knockout mutants (Additional

file 2: Figure S4). Conversely, the level of *PINRT2* transcript was elevated in the *PIANK1* knockout mutants in both the early and late infection stages (Additional file 2: Figure S4).

To further examine whether nitrogen assimilation was affected by *PIANK1*, the nitrogen utilization capabilities of WT, KO11, and KO39 were compared by measuring their growth on Plich media with different organic and inorganic nitrogen sources. Compared with WT, the *PIANK1* knockout mutants exhibited higher growth inhibition rates on Plich media containing  $\text{NO}_3^-$ ,  $\text{NO}_2^-$ , or  $\text{NH}_4^+$  as the single inorganic nitrogen source (Fig. 7c, d). However, the growth of KO11 and KO39 was not affected when glutamine was used as an organic nitrogen source, and even showed a lower inhibition rate when proline was used (Fig. 7c, d). Given that the growth of the *PIANK1* knockout mutants was not affected on the media containing organic nitrogen sources, we performed an inoculation assay again with the addition of

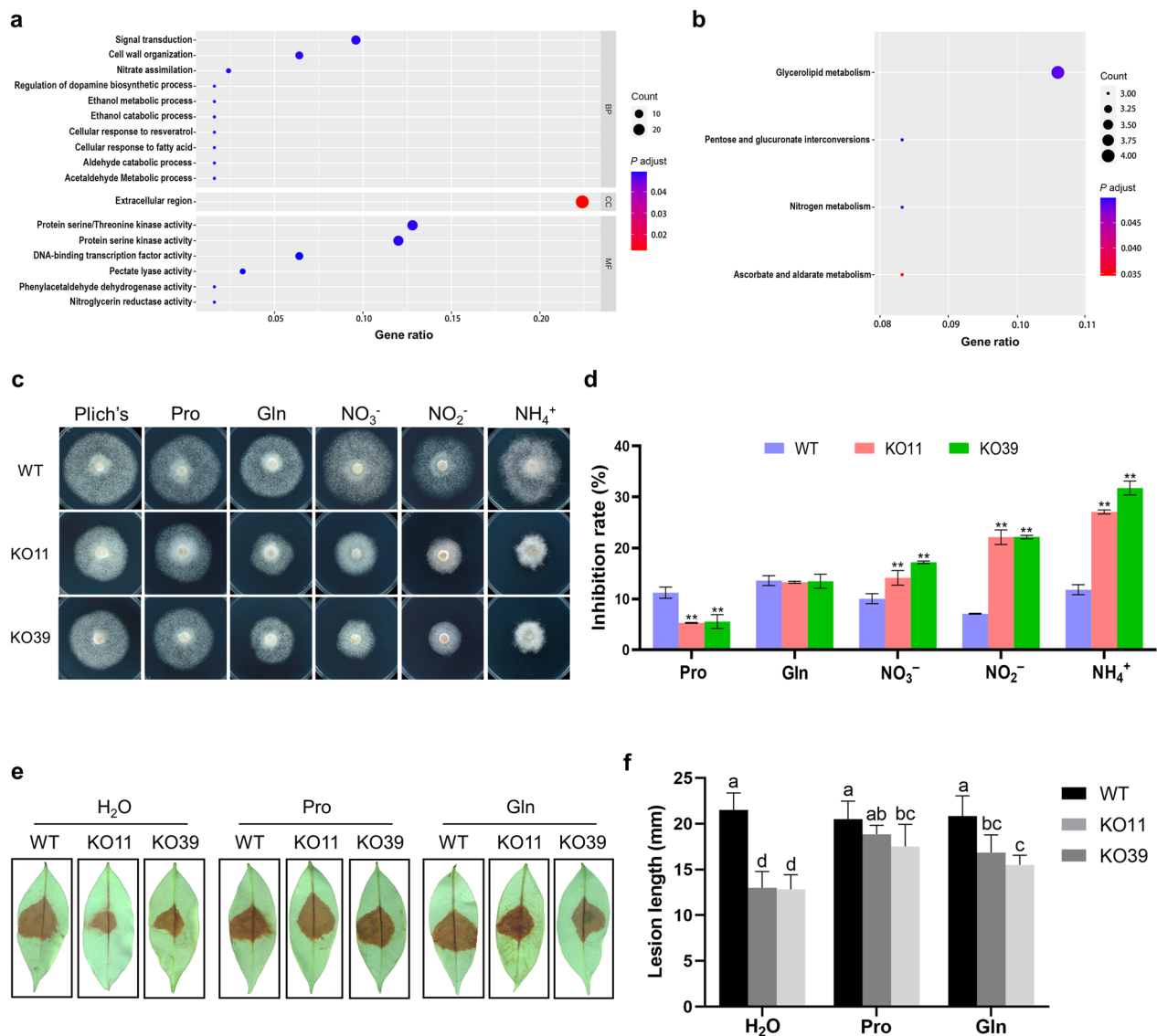


**Fig. 7** *PIANK1* regulates the nitrogen assimilation pathway in *Peronophythora litchii*. **a** and **b** Gene ontology and KEGG enrichment analysis of the DEGs. **c** The WT, KO11, and KO39 strains were grown for 7 d on Plich medium or defined media with  $\text{NO}_3^-$ ,  $\text{NO}_2^-$ , and  $\text{NH}_4^+$ , glutamine (Gln) and proline (Pro). **d** Inhibition rates from the above colonies at 7 d post-inoculation. Data represent means  $\pm$  SD. The experiment was repeated three times independently, with three technical replications per biological repeat. Asterisks denote significant differences between the *PIANK1* knockout mutants and WT strain (\*\* $p < 0.01$ ). **e** The application of Pro and Gln in the infection stage. Zoospore suspension containing 10 mM Pro or Gln was inoculated on litchi leaves ( $n > 12$  for each strain) for 36 h at 25 °C in the dark. **f** Lesion length measured after 36 hpi. Different letters represent significant differences ( $p < 0.01$ ; Duncan's Multiple Range Test). The experiment was repeated three times independently

exogenous proline and glutamine. The results showed that the application of proline and glutamine can partially restore the infection process of the *PIANK1* deletion mutants (Fig. 7e, f). The above results suggest that *PIANK1* regulates the growth and virulence of *P. litchii* by affecting pathogen nitrate assimilation.

## Discussion

Ankyrin (ANK) repeats, known to mediate protein-protein interactions, is a ubiquitous protein structural domain distributed in diverse organisms ranging from viruses to humans. Although ANK-containing proteins perform a wide range of functions in animals, yeasts, and plants (Manik et al. 2017; Tyrkalska et al. 2017; Lindsay

et al. 2022; Tang et al. 2022), little is known about their functions in oomycetes. In this study, we systematically identified the genes encoding ANK-containing proteins in the litchi pathogen *P. litchii* and found that *PLANK1*, of these genes, plays critical roles in vegetative growth, zoospore encystment, cyst germination, stress responses, oospore development, and virulence of *P. litchii*. The orthologs of *PLANK1* were exclusive to oomycete species, suggesting a potentially oomycete-specific function. Further experiments revealed that *PLANK1* regulates *P. litchii* growth and virulence by affecting pathogen nitrate assimilation. However, considering the growth defects caused by the absence of *PLANK1*, whether *PLANK1* regulates the pathogen infection process directly should be further investigated.

The number of ANK-containing proteins in *Arabidopsis*, rice, maize, and soybean is 105, 175, 71, and 226, respectively (Becerra et al. 2004; Huang et al. 2009; Jiang et al. 2013; Zhao et al. 2020). There are 284 ANK-containing proteins in *P. litchii*, more than in plants. We further identified ANK-containing proteins in other phytopathogenic oomycetes and *F. graminearum* (Additional file 1: Table S4). Intriguingly, the numbers of ANK-containing proteins in phytopathogenic oomycetes are between 200 and 500, significantly higher than in plants and fungi. This result indicated that the genes encoding ANK-containing proteins in phytopathogenic oomycetes rapidly expanded during evolution. Gene duplication is one of the vital driving forces in the evolution of genomes and genetic systems (Moore et al. 2003). In rice, the *OsANK* genes arranged in tandem were much larger than those involved in segmental duplication events, suggesting that tandem duplications might have played a key role in the expansion of the *OsANK* gene family (Huang et al. 2009). How these *PLANK* genes expanded in *P. litchii* and other oomycetes needs further analysis. In addition, ANK-containing proteins are usually clustered into different subfamilies based on domain compositions. Except for the subfamily ANK-M, which consists of proteins with only ankyrin repeat, 24 members with the transmembrane domain were identified in *P. litchii*. The transmembrane domain is the most common domain found in *P. litchii* ANK-containing proteins, which is consistent with previous reports in plants (Becerra et al. 2004; Huang et al. 2009; Jiang et al. 2013; Zhao et al. 2020). However, the functions of ANK-transmembrane proteins are still largely unknown and worth studying in the future.

Since ANK-containing proteins appear to be conserved in structure rather than in function (Li et al. 2006), the expression profile of the *PLANK* genes may provide clues to their functions. A study of *F. graminearum* found that NO was produced in *F. graminearum* in response to host signals at the pre-contact stage by transcriptome analysis

(Ding et al. 2020). *FgANK1*, one of the top differentially expressed genes at the pre-contact stage, was demonstrated to be required for host-mediated NO production and virulence in *F. graminearum* (Ding et al. 2020). Our RNA-Seq data showed that 183 (64%) *PLANK* genes were differentially expressed during litchi-*P. litchii* interaction (Fig. 1a and Additional file 1: Table S1). Here, we demonstrated that one of the up-regulated genes, *PLANK1*, was involved in the pathogen's virulence. However, among the differentially expressed *PLANK* genes, 66% of them were down-regulated in this process, indicating that most ANK-containing proteins might have a negative role during the pathogen infection.

Nitrogen assimilation plays a vital role in obtaining nitrogen for amino acid biosynthesis in organisms (Lam et al. 1996). In this study, we found that *PLANK1* was involved in nitrogen assimilation. The *PLANK1* knockout mutants exhibited reduced efficiency in utilizing  $\text{NO}_3^-$ ,  $\text{NO}_2^-$ , and  $\text{NH}_4^+$ , which may cause inadequate ammonium conversion to amino acids, such as glutamate. In fungi, extracellular nitrate is transported into cells by the nitrate transporter, metabolized by nitrate reductase to nitrite, and then converted to ammonium via nitrite reductase (Lapp et al. 2014; Tang et al. 2020). Therefore, the growth arrest of the *PLANK1* knockout mutants on the media amended with  $\text{NO}_3^-$ ,  $\text{NO}_2^-$ , and  $\text{NH}_4^+$  may be due to the down-regulation of *PINRT1*, *PINRT2*, and *PINiR1*. Intriguingly, *PINRT2* showed a higher expression level in the *PLANK1* deletion mutants during the infection stages (Additional file 2: Figure S4). Thus, other unidentified components may be controlling the expression of *PINRT2* to compensate for the nitrogen assimilation defect in the infection stages. Alternatively, *PINRT2* may be negatively regulated by *PLANK1* in the infection stages, depending on the environmental nitrogen source concentration or other conditions. Exogenously supplied proline and glutamine can partially restore the virulence of *PLANK1* deletion mutants, indicating the vital role of nitrogen assimilation in pathogen infection. The nitrate transporter gene is physically linked to and coregulated with the genes encoding nitrate reductase and nitrite reductase in *P. infestans* (Abrahamian et al. 2016). Silencing of all three nitrate assimilation genes results in loss of pathogen virulence on potato leaves but colonizing tubers (Abrahamian et al. 2016). Thus, determining how *PLANK1* regulates the nitrogen assimilation pathway will improve our understanding of the oomycete pathogenic mechanism.

Sexual reproduction is a critical process in the pathogenic life cycle of oomycetes, as the resulting sexual oospores can survive in soil or debris for several years (Babadoost et al. 2013; Feng et al. 2023). However, our understanding of the molecular mechanisms of oomycete

sexual reproduction lagged for many years because of the lack of genome editing technologies and functional genomic studies. The first gene reported to mediate *P. litchii* oospore formation was *PLM90*, which encodes a Puf RNA-binding protein. The silencing of *PLM90* led to a significant decline in oospore production (Jiang et al. 2017). A recent study of M90 in *P. ultimum* further found that PuM90 could repress PuFLP mRNA level via binding to the 3' untranslated region of PuFLP, thereby facilitating oospore formation (Feng et al. 2021). The C<sub>2</sub>H<sub>2</sub> zinc finger transcription factor CZF1 also mediated oospore development in *P. sojae* and *P. litchii* (Wang et al. 2009; Zhu et al. 2022). Whether oospore development regulated by *PLANK1* is related to these proteins should be tested in future studies. Besides, the deletion of *PLNRT1*, *PLNRT2*, or *PLNiR1* should be conducted to verify the link between nitrogen assimilation and oospore development.

## Conclusions

In this study, we identified 284 non-redundant genes encoding ANK-containing proteins in *P. litchii*, which were classified into 11 subfamilies. Further experiments found that *PLANK1* was a positive regulator of vegetative growth, zoospore development, cyst germination, stress tolerance, and virulence in *P. litchii*. Moreover, the *PLANK1* deletion mutants abolished the ability of *P. litchii* to generate normal oospores, indicating its critical role in this sexual reproduction. Through transcriptomic analysis and nitrogen source utilization assays, we demonstrated that *PLANK1* mediates the pathogen's nitrogen metabolism. This study is the first report on the identification of ANK-containing proteins in oomycetes and the characterization of the biological function of one such protein. These findings open a new avenue for understanding the molecular mechanisms underlying oospore development and virulence in phytopathogenic oomycetes.

## Methods

### Identification of *P. litchii* ANK-containing proteins

We obtained the Hidden Markov Model (HMM) profile of the ANK motif (PF13637) from InterPro (<https://www.ebi.ac.uk/interpro/>). BLAST was used to identify putative ANK-containing proteins with the ANK motif (PF13637) as a query against the *P. litchii* predicted protein database. The redundant sequences were removed manually. Then, all candidate sequences that met the standards were checked manually using the SMART program (<http://smart.embl-heidelberg.de/>) and predicted the conserved domain other than the ANK motif. Signal peptides were predicted by SignalP-5.0 (<https://services.healthtech.dtu.dk/service.php?SignalP-5.0>).

### Phylogenetic analysis

Sequence alignment (Muscle algorithm) and phylogenetic tree were constructed with the Neighbor-Joining algorithm with 1000 bootstrap replications in the MEGA X program.

### Microbial strains and culture conditions

*Peronophythora litchii* strain SHS3 was isolated from the infected litchi fruit and maintained in the mycological laboratory of the Department of Plant Pathology, South China Agricultural University, China. The strain was cultured on CA medium (juice from 200 g carrot topped up to 1 L, 15 g/L agar for solid medium) at 25 °C in the dark. *Escherichia coli* DH5 $\alpha$  was cultured at 37 °C in Luria Bertani (LB) medium (86 mM NaCl, 10 g/L peptone, 5 g/L yeast extract, 15 g/L agar for solid medium) and used for the cloning and propagation of recombinant plasmids.

### RNA extraction and gene expression analysis

For expression profile analysis, mycelia, sporangia, zoospores, cysts, germinating cysts, oospores, and litchi leaves infected with zoospore suspension of *P. litchii* were harvested at the indicated time points, and RNA was extracted using All-In-One DNA/RNA Mini-preps Kit (Bio Basic, Markham, Canada) according to the recommended protocol. All cDNAs were synthesized from total RNA by PrimeScript RT Master Mix (Takara, Shiga, Japan). qPCR was performed in 20  $\mu$ L reactions that included 20 ng cDNA, 0.4  $\mu$ M gene-specific primer, 10  $\mu$ L SYBR Premix ExTaq II (Takara, Shiga, Japan) and 6.4  $\mu$ L ddH<sub>2</sub>O. The qPCR was performed on qTOWER3 Real-Time PCR thermal cyclers (Analytik Jena, Jena, Germany) under the following conditions: 95 °C for 2 min, 40 cycles at 95 °C for 30 s, and 60 °C for 30 s to calculate cycle threshold values, followed by a dissociation program of 95 °C for 15 s, 60 °C for 1 min, and 95 °C for 15 s to obtain melt curves. The relative expression values were determined using *PLActin* as the reference gene and calculated with the 2<sup>- $\Delta\Delta$ Ct</sup> method.

### Plasmid construction and CRISPR-mediated gene knockout

All the primers used in this study are listed in Additional file 1: Table S5. The PCR fragments were amplified by Phanta Max Super-Fidelity DNA Polymerase (Vazyme, Nanjing, China). The deletion of *PLANK1* was conducted by the CRISPR-mediated gene replacement strategy. The CRISPR-mediated knockout plasmid pYF2.3G-RibosgRNA and the donor DNA plasmid pBS-SK II+ that contained the 1 kb of homology arms surrounding the *PLANK1* gene were generated as described previously (Fang et al., 2016). For *PLANK1* complementation, the entire gene-coding region with mutated sgRNA sites was linked to the linearized pTORMGFP, which was digested

by ClaI and BsiWI (New England Biolabs, Hitchin, UK). Transformation of the *P. litchii* strain SHS3 was performed as described previously (Situ et al. 2020).

### Sensitivity to various stresses and nitrogen source utilization assays

To test the stress tolerance, the mycelial plugs of the WT, CK, *PIANK1* knockout mutant, and complementation strains were grown on Plich media containing 0.05 M NaCl, 0.1 M CaCl<sub>2</sub>, 0.2 M D-sorbitol, 2 mM H<sub>2</sub>O<sub>2</sub>, 100 µg/mL CFW, or 350 µg/mL CR for 7 d. For growth tests on different nitrogen sources, all strains were cultured on Plich media with the following nitrogen sources: nitrate (NO<sup>3-</sup>, 10 mM), nitrite (NO<sup>2-</sup>, 0.1 mM), ammonium (NH<sup>4+</sup>, 10 mM), glutamine (Gln, 10 mM), and proline (Pro, 10 mM). The inhibition rate was calculated as follows: Inhibition rate (%) = [(the average colony diameter on Plich – the average colony diameter on Plich with a stress agent or different nitrogen sources) / the average colony diameter on Plich] × 100. All the experiments were repeated three times, with three replicates each time.

### Methylthiazolyldiphenyl-tetrazolium bromide staining

Methylthiazolyldiphenyl-tetrazolium bromide (MTT) staining was performed by mixing the oospore suspension with equivalent volumes of 0.1% MTT (Sigma-Aldrich, St. Louis, USA) in 0.1 M PBS (pH 5.8), and incubated at 37 °C for 24 h before observing under an Olympus BX53 microscope (Olympus, Tokyo, Japan). The red or purple oospores were considered dormant viable, whereas the black and unstained oospores were non-viable (Guo et al. 2017).

### Inoculation assays

Inoculation assays were performed by inoculating *P. litchii* on the tender leaves or fruit (70% ripening stage) of litchi (cv. 'Feizixiao'), which were collected from the litchi orchard in South China Agricultural University, Guangzhou, Guangdong province. For zoospore inoculation, 100 zoospores of each strain were inoculated on the center of the tender leaf or fruit and kept at 80% humidity in 12 h-light/12 h-darkness at 25 °C. For mycelial mat inoculation, a mycelial mat of each strain was inoculated on the center of the tender leaf or fruit. Each strain was tested on at least 30 leaves or fruit. The symptoms were observed, and the lesion diameter was measured at 48 hpi. The experiments were repeated at least three times.

### Abbreviations

ANK	Ankyrin repeat
CA	Carrot juice agar
CFW	Calcofluor white

CR	Congo red
DEGs	Differentially expressed genes
GO	Gene ontology
KEGG	Kyoto encyclopedia of genes and genomes
MTT	Methylthiazolyldiphenyl-tetrazolium bromide

### Supplementary Information

The online version contains supplementary material available at <https://doi.org/10.1186/s42483-023-00211-y>.

**Additional file 1: Table S1.** The amino acid and transcriptional feature of *PIANK* proteins. **Table S2.** The sequence of the *hygromycin B* gene optimized for *Peronophthora litchii* expression. **Table S3.** DEGs in RNA-Seq data of *PIANK1* knockout mutants. **Table S4.** The number of ANK-containing proteins in different oomycetes and fungus. **Table S5.** Primers used in this study.

**Additional file 2: Figure S1.** Number of ANK motifs in *PIANK* proteins. The number of ANK motifs in a protein was predicted by Pfam analysis (PF13637). **Figure S2.** Expression profile of *PIANK1*. Relative expression levels of *PIANK1* were determined by RT-qPCR with total RNA extracted from mycelia (MY), sporangia (SP), zoospores (ZO), cysts (CY), germinating cysts (GC), and oospores (OO), samples from 1.5, 3, 6, 12, and 24 h post-inoculation of tender litchi leaves with zoospores. The constitutive expression of *PIActin* was used as a reference gene, and expression levels were normalized using the MY values as 1. The experiment was repeated three times with independent sampling. **Figure S3.** Inoculation assay of *PIANK1* knockout mutants inoculated by mycelial mats. **a** Mycelial mats of the WT, CK, and *PIANK1* knockout mutants and complemented strain were inoculated on tender litchi leaves ( $n > 30$  for each strain) for 48 h at 25 °C in the dark. Images are two representatives for each instance. **b** Lesion length measured after 48 hpi. Different letters represent significant differences ( $p < 0.01$ ; Duncan's Multiple Range Test). **c** Mycelial mats of the WT, CK, and *PIANK1* knockout mutant and complementation strains were inoculated on litchi fruit ( $n > 30$  for each strain) for 72 h at 25 °C in the dark. Images are three representatives for each instance. **d** Lesion length measured after 72 hpi. Different letters represent significant differences ( $p < 0.01$ ; Duncan's Multiple Range Test). Experiments were repeated three times independently. **Figure S4.** RT-qPCR analysis to validate the nitrogen assimilation pathway genes in mycelia and infection stages of *Peronophthora litchii*. The constitutive expression of *PIActin* was used as a reference gene, and expression levels were normalized using the WT values as 1. Data represent means ± SD. The experiment was repeated three times with independent sampling. Asterisks denote significant differences between the *PIANK1* knockout mutants and the WT strain (\*\*  $p < 0.01$ ).

### Acknowledgements

Not applicable.

### Author contributions

ZJ and JS designed experiments, JS and XZ performed the experiments, JS, XZ, XFZ, ZZ, PX, and GK analyzed the data, JS, XZ, and XFZ wrote the manuscript. All authors read and approved the final manuscript.

### Funding

This work was supported by the earmarked fund for China Agriculture Research System (CARS-32).

### Availability of data and materials

Not applicable.

### Declarations

### Ethics approval and consent to participate

Not applicable.

### Consent for publication

Not applicable.

**Competing interests**

The authors declare that they have no competing interests.

Received: 6 July 2023 Accepted: 26 October 2023

Published online: 05 December 2023

**References**

- Abrahamian M, Ah-Fong AM, Davis C, Andreeva K, Judelson HS. Gene expression and silencing studies in *Phytophthora infestans* reveal infection-specific nutrient transporters and a role for the nitrate reductase pathway in plant pathogenesis. *PLoS Pathog*. 2016;12:e1006097. <https://doi.org/10.1371/journal.ppat.1006097>.
- Al-Khodor S, Price CT, Kalia A, Abu KY. Functional diversity of ankyrin repeats in microbial proteins. *Trends Microbiol*. 2010;18:132–9. <https://doi.org/10.1016/j.tim.2009.11.004>.
- Babadoost M, Pavon C. Survival of oospores of *Phytophthora capsici* in soil. *Plant Dis*. 2013;97:1478–83. <https://doi.org/10.1094/PDIS-12-12-1123-RE>.
- Beakes GW, Glockling SL, Sekimoto S. The evolutionary phylogeny of the oomycete “fungi.” *Protoplasma*. 2012;249:3–19. <https://doi.org/10.1007/s00709-011-0269-2>.
- Becerra C, Jahrmann T, Puigdomenech P, Vicent CM. Ankyrin repeat-containing proteins in Arabidopsis: characterization of a novel and abundant group of genes coding ankyrin-transmembrane proteins. *Gene*. 2004;340:111–21. <https://doi.org/10.1016/j.gene.2004.06.006>.
- Breedon L, Nasmyth K. Similarity between cell-cycle genes of budding yeast and fission yeast and the Notch gene of *Drosophila*. *Nature*. 1987;329:651–4. <https://doi.org/10.1038/329651a0>.
- Ding Y, Gardiner DM, Xiao D, Kazan K. Regulators of nitric oxide signaling triggered by host perception in a plant pathogen. *Proc Natl Acad Sci USA*. 2020;117:11147–57. <https://doi.org/10.1073/pnas.1918977117>.
- Fang YF, Tyler BM. Efficient disruption and replacement of an effector gene in the oomycete *Phytophthora sojae* using CRISPR/Cas9. *Mol Plant Pathol*. 2016;17:127–39. <https://doi.org/10.1111/mpp.12318>.
- Feng H, Wan CX, Zhang ZC, Chen H, Li ZP, Jiang HB, et al. Specific interaction of an RNA-binding protein with the 3'-UTR of its target mRNA is critical to oomycete sexual reproduction. *PLoS Pathog*. 2021;17:e1010001. <https://doi.org/10.1371/journal.ppat.1010001>.
- Feng H, Liu TL, Li JX, Wan CX, Ding FF, Wang YC, et al. Gene editing with an oxathiapiprolin resistance selection marker reveals that PuLLP, a loricrin-like protein, is required for oospore development in *Pythium ultimum*. *Phytopathol Res*. 2023;5:34. <https://doi.org/10.1186/s42483-023-00189-7>.
- Huang JY, Zhao XB, Yu HH, Ouyang YD, Wang L, Zhang QF. The ankyrin repeat gene family in rice: genome-wide identification, classification and expression profiling. *Plant Mol Biol*. 2009;71:207–26. <https://doi.org/10.1007/s11103-009-9518-6>.
- Jiang HY, Wu QQ, Jin J, Sheng L, Yan HW, Cheng BJ, et al. Genome-wide identification and expression profiling of ankyrin-repeat gene family in maize. *Dev Genes Evol*. 2013;223:303–18. <https://doi.org/10.1007/s00427-013-0447-7>.
- Jiang LQ, Ye WW, Situ JJ, Chen YB, Yang XY, Kong GH, et al. A Puf RNA-binding protein encoding gene *PIM90* regulates the sexual and asexual life stages of the litchi downy blight pathogen *Peronophythora litchii*. *Fungal Genet Biol*. 2017;98:39–45. <https://doi.org/10.1016/j.fgb.2016.12.002>.
- Guo T, Wang XW, Shan K, Sun WX, Guo LY. The Loricrin-like protein (LLP) of *Phytophthora infestans* is required for oospore formation and plant infection. *Front Plant Sci*. 2017;8:142. <https://doi.org/10.3389/fpls.2017.00142>.
- Kamoun S, Furzer O, Jones JDG, Judelson HS, Ali GS, Dalio RJD, et al. The top 10 oomycete pathogens in molecular plant pathology. *Mol Plant Pathol*. 2015;16:413–34. <https://doi.org/10.1111/mpp.12190>.
- Kolodziej MC, Singla J, Sánchez-Martín J, Zbinden H, Šimková H, Karafiátová M, et al. A membrane-bound ankyrin repeat protein confers race-specific leaf rust disease resistance in wheat. *Nat Commun*. 2021;12:956. <https://doi.org/10.1038/s41467-020-20777-x>.
- Kumar A, Balbach J. Folding and stability of ankyrin repeats control biological protein function. *Biomolecules*. 2021;11:840. <https://doi.org/10.3390/biom11060840>.
- Lam HM, Coschigano KT, Oliveira IC, Melo-Oliveira R, Coruzzi GM. The molecular-genetics of nitrogen assimilation into amino acids in higher plants. *Annu Rev Plant Biol*. 1996;47:569–93. <https://doi.org/10.1146/annurev.arplant.47.1.569>.
- Lapp K, Vödisch M, Kroll K, Strassburger M, Kniemeyer O, Heinekamp T, et al. Characterization of the *Aspergillus fumigatus* detoxification systems for reactive nitrogen intermediates and their impact on virulence. *Front Microbiol*. 2014;5:469.
- Li JN, Mahajan A, Tsai MD. Ankyrin repeat: a unique motif mediating protein–protein interactions. *Biochemistry*. 2006;45:15168–78. <https://doi.org/10.1021/bi062188q>.
- Li W, Li P, Zhou XF, Situ JJ, Lin YM, Qiu JH, et al. A cytochrome B-5-like heme/steroid binding domain protein, PICB5L1, regulates mycelial growth, pathogenicity and oxidative stress tolerance in *Peronophythora litchii*. *Front Plant Sci*. 2021;12:783438. <https://doi.org/10.3389/fpls.2021.783438>.
- Lindsay PL, Ivanov S, Pumplin N, Zhang XC, Harrison MJ. Distinct ankyrin repeat subdomains control VAPYRIN locations and intracellular accommodation functions during arbuscular mycorrhizal symbiosis. *Nat Commun*. 2022;13:5228. <https://doi.org/10.1038/s41467-022-32124-3>.
- Lux SE, John KM, Bennett V. Analysis of cDNA for human erythrocyte ankyrin indicates a repeated structure with homology to tissue-differentiation and cell-cycle control proteins. *Nature*. 1990;344:36–42. <https://doi.org/10.1038/344036a0>.
- Manik MK, Yang H, Tong J, Im YJ. Structure of yeast OSBP-related protein Osh1 reveals key determinants for lipid transport and protein targeting at the nucleus-vacuole junction. *Structure*. 2017;25:617–29. <https://doi.org/10.1016/j.str.2017.02.010>.
- Moore RC, Purganan MD. The early stages of duplicate gene evolution. *Proc Natl Acad Sci USA*. 2003;100:15682–7. <https://doi.org/10.1073/pnas.2535513100>.
- Odon V, Georgana I, Holley J, Morata J, de Motes CM. Novel class of viral ankyrin proteins targeting the host E3 ubiquitin ligase cullin-2. *J Virol*. 2018;92:e01374-e1418. <https://doi.org/10.1128/JVI.01374-18>.
- Pedley KF, Walton JD. Regulation of cyclic peptide biosynthesis in a plant pathogenic fungus by a novel transcription factor. *Proc Natl Acad Sci USA*. 2001;98:14174–9. <https://doi.org/10.1073/pnas.231491298>.
- Sedgwick SG, Smerdon SJ. The ankyrin repeat: a diversity of interactions on a common structural framework. *Trends Biochem Sci*. 1999;24:311–6. [https://doi.org/10.1016/S0968-0004\(99\)01426-7](https://doi.org/10.1016/S0968-0004(99)01426-7).
- Sharma N, Bham K, Senapati S. Human ankyrins and their contribution to disease biology: an update. *J Biosci*. 2020;45:146. <https://doi.org/10.1007/s12038-020-00117-3>.
- Situ JJ, Jiang LQ, Fan XN, Yang WS, Li W, Xi PG, et al. An RXLR effector PIAvH142 from *Peronophythora litchii* triggers plant cell death and contributes to virulence. *Mol Plant Pathol*. 2020;21:415–28. <https://doi.org/10.1111/mpp.12905>.
- Situ JJ, Xi PG, Lin L, Huang WX, Song Y, Jiang ZD, et al. Signal and regulatory mechanisms involved in spore development of *Phytophthora* and *Peronophythora*. *Front Microbiol*. 2022;13:984672. <https://doi.org/10.3389/fmicb.2022.984672>.
- Tang C, Li TY, Klosterman SJ, Tian CM, Wang YL. The bZIP transcription factor VdAtf1 regulates virulence by mediating nitrogen metabolism in *Verticillium dahliae*. *New Phytol*. 2020;226:1461–79. <https://doi.org/10.1111/nph.16481>.
- Tang Q, Zhao YN, Luo S, Lu S. AKR2A is involved in the flowering process of *Arabidopsis thaliana*. *Plant Signal Behav*. 2022;17:2100685. <https://doi.org/10.1080/15592324.2022.2100685>.
- Thines M. Phylogeny and evolution of plant pathogenic oomycetes—a global overview. *Eur J Plant Pathol*. 2014;138:431–47. <https://doi.org/10.1007/s10658-013-0366-5>.
- Tyrkalska SD, Candel S, Perez-Oliva AB, Valera A, Alcaraz-Perez F, Garcia-Moreno D, et al. Identification of an evolutionarily conserved ankyrin domain containing protein, Caiap, which regulates inflammasome-dependent resistance to bacterial infection. *Front Immunol*. 2017;8:1–16. <https://doi.org/10.3389/fimmu.2017.01375>.
- Wang H, Zou SH, Li YW, Lin FY, Tang DZ. An ankyrin-repeat and WRKY-domain-containing immune receptor confers stripe rust resistance

- in wheat. *Nat Commun.* 2020;11:1353. <https://doi.org/10.1038/s41467-020-15139-6>.
- Wang JR, Zhou GQ, Huang WX, Li W, Feng DN, Liu LC, et al. Autophagy-related gene *PIATG6a* is involved in mycelial growth, asexual reproduction and tolerance to salt and oxidative stresses in *Peronophythora litchii*. *Int J Mol Sci.* 2022;23:1839. <https://doi.org/10.3390/ijms23031839>.
- Wang YL, Dou DL, Wang XL, Li AN, Sheng YT, Hua CL, et al. The *PscZF1* gene encoding a C<sub>2</sub>H<sub>2</sub> zinc finger protein is required for growth, development and pathogenesis in *Phytophthora sojae*. *Microb Pathog.* 2009;47:78–86. <https://doi.org/10.1016/j.micpath.2009.04.013>.
- Ye WW, Wang Y, Shen DY, Li DL, Pu THZ, Jiang ZD, et al. Sequencing of the litchi downy blight pathogen reveals it is a *Phytophthora* species with downy mildew-like characteristics. *Mol Plant-Microbe Interact.* 2016;29:573–83. <https://doi.org/10.1094/MPMI-03-16-0056-R>.
- Zhang FJ, Xie YH, Jiang H, Wang X, Hao YJ, Zhang ZL, et al. The ankyrin repeat-containing protein MdANK2B regulates salt tolerance and ABA sensitivity in *Malus domestica*. *Plant Cell Rep.* 2021;40:405–19. <https://doi.org/10.1007/s00299-020-02642-9>.
- Zhao JY, Lu ZW, Sun Y, Fang ZW, Chen J, Zhou YB, et al. The ankyrin-repeat gene *GmANK114* confers drought and salt tolerance in *Arabidopsis* and Soybean. *Front Plant Sci.* 2020;11:584167. <https://doi.org/10.3389/fpls.2020.584167>.
- Zhu HH, Situ JJ, Guan TF, Dou ZY, Kong GH, Jiang ZD, et al. A C<sub>2</sub>H<sub>2</sub> zinc finger protein PICZF1 is necessary for oospore development and virulence in *Peronophythora litchii*. *Int J Mol Sci.* 2022;23:2733. <https://doi.org/10.3390/ijms23052733>.

Ready to submit your research? Choose BMC and benefit from:

- fast, convenient online submission
- thorough peer review by experienced researchers in your field
- rapid publication on acceptance
- support for research data, including large and complex data types
- gold Open Access which fosters wider collaboration and increased citations
- maximum visibility for your research: over 100M website views per year

At BMC, research is always in progress.

Learn more [biomedcentral.com/submissions](https://biomedcentral.com/submissions)

